PERGAMON

International Journal of Heat and Mass Transfer 44 (2001) 3565–3573

International Journal of HEAT and MASS TRANSFER

www.elsevier.com/locate/ijhmt

A comparative study of compact enhanced fin-and-tube heat exchangers

Chi-Chuan Wang [a,*], Wei-Song Lee [b], Wen-Jenn Sheu [b]

[a] *Energy and Resources Laboratories, Industrial Technology Research Institute, D400 ERL/ITRI, Bldg. 64, 195-6 Section 4, Chung Hsing Road, Chutung, Hsinchu 310, Taiwan, ROC*

[b] *Department of Power Mechanical Engineering, National Tsin Hua University, Hsinchu 300, Taiwan, ROC*

Received 22 September 2000

Abstract

Experimental study on the airside performance of compact slit fin-and-tube heat exchangers was carried out. Test results indicated the airside performance for compact slit fin geometry is relatively independent of the number of tube row and fin pitch. The results are quite different from previous studies concerning the slit fin geometry. This may be attributable to a smaller slit breadth of this study. Test results of the present slit fin were compared with louver fin and plain fin using various comparison methods. In all cases, the relevant airside performance of the interrupted surfaces (including louver and slit) is superior to that of plain fin surface. However, it should be pointed out that the associated superiority may decrease with decreasing fin pitch and Reynolds number. An updated correlation of the airside performance for the slit fin geometry describing 56 test samples is proposed. The mean deviation of the proposed heat transfer correlation is 7.26% and is 7.18% for frictional correlation.

1. Introduction

For an air-cooled heat exchanger, the dominant thermal resistance is usually on the air side. Therefore, to effectively reduce the airside resistance for saving energy and resources, manufacturers of heat exchangers seek to enhance the airside performance. This includes the use of smaller heat transfer tube, smaller transverse tube pitch, and smaller longitudinal tube pitch. Benefits of using smaller diameter tubes includes smaller form drag caused by the tube, higher heat transfer coefficients due to smaller hydraulic diameter, and less refrigerant inventory into the system. In this connection, the tube size for the residential air-conditioning system shows a substantial decrease in recent years from 9.52, 7.94, to 7 mm. Furthermore, enhanced surfaces like wavy, slit and louver are usually accompanied with the reduction of tube size for better overall performance. This eventually introduces a very effective and compact heat exchangers. The most frequent interrupted surfaces take the form as louver and slit fin surfaces as depicted in Fig. 1.

Performance data of the fin-and-tube heat exchangers is very important for accurate design. However, airside performance is usually considered proprietary. Recently, a thorough review of the recent progress about the airside performance was summarized by Wang [1]. For louver fin geometry, Wang et al. [2] had proposed a generalized airside correlation based on their extensive test data. In comparison with the louver fin geometry, test results of slit fin geometry are comparatively fewer. The only papers related to this subject were by Nakayama and Xu [3], Wang et al. [4] and Du and Wang [5]. However, it seems that the previous studies were mainly focused on larger tube diameter and larger longitudinal and transverse tube pitch. In addition, detailed comparisons of the slit fin geometry to other fin patterns were not made. As a consequence, the objective of this is to report new experimental data related to 7-mm slit geometry and relevant comparisons with other fin geometry.

* Corresponding author. Tel.: +886-3-591-6294; fax: +886-3-582-0250.

E-mail address: ccwang@itri.org.tw (C.-C. Wang).

0017-9310/01/$ - see front matter
PII: S0017-9310(01)00011-4

Nomenclature

A_c	minimum flow area, (m^2)
A_d^*	relative frontal area
A_o	total surface area, (m^2)
Cp	specific heat, (J kg^{-1} K)
D_c	fin collar outside diameter, (m)
d, D_h	hydraulic diameter, $4A_cL/A_o$, (m)
E	friction power expended per unit of surface area, (W m^{-2})
f	friction factor, dimensionless
$f1, f2, f3, f4, f5, f6$	correlation parameter
F_p	fin pitch, (m)
F_s	fin spacing, (m)
G_c	mass flux based on minimum flow area, (kg m^{-2} s^{-1})
g_c	conversion factor, 1 kg m N^{-1} s^{-2}
h	heat transfer coefficient, (W m^{-2} K^{-1})
j	$Nu/RePr^{1/3}$, the Colburn factor, dimensionless
$j1, j2, j3, j4, j5, j6, j7$	correlation parameter
L	depth of the heat exchanger, (m)
S_n	number of slits in an enhanced zone, dimensionless
N	number of longitudinal tube rows, dimensionless
Nu	Nusselt number, dimensionless
P_d^*	relative pumping power
P_l	longitudinal tube pitch, (m)
P_t	transverse tube pitch, (m)
Pr	Prandtl number, dimensionless
Re_{Dh}	Reynolds number based on hydraulic diameter, G_cD_h/μ_{air} dimensionless
Re_{Dc}	Reynolds number based on tube collar diameter, G_cD_c/μ_{air}, dimensionless
S_h	height of slit, (m)
S_s	breadth of a slit in the direction of airflow, (m)
S_w	width of slit, (m)
V_d^*	relative volume
δ_f	fin thickness, (m)
β	ratio of total transfer area on one side of the exchanger to total volume of the exchanger, $4\sigma/D_h$, (m^{-1})
σ	contraction ratio of the fin array, dimensionless
μ	dynamic viscosity of fluid, (N s m^{-2})
ρ	mass density of fluid, (kg m^{-3})
η_o	surface efficiency

2. Experimental apparatus and reduction methods

In this study, a total of six samples of fin-and-tube heat exchangers having slit geometry was investigated in the present study ($D_c = 7.6$ mm, $P_t = 21$ mm, $P_l = 12.7$ mm). Their related geometric parameters are tabulated in Table 1. For comparison purpose, related geometries of previous investigators are also included. Detailed dimensions of the slit fin patterns are illustrated in Fig. 1(a). The present fin possesses an offset slit geometry.

For the sake of simplicity, detailed description of the test facility and the related reduction method of the heat transfer performance are omitted, one can find the associated details from previous investigations [6,7]. Tests were performed in fully dry test conditions. Uncertainties of the Colburn j factor and friction factor f were estimated, by the method suggested by Moffat [8], ranging from 2.2% to 13.1% for the j factors, and 3.0–16.6% for f. The highest uncertainties were associated with lowest Reynolds number.

3. Results and discussion

Fig. 2 shows the test results for the present compact slit fin geometry. The number of tube rows are 1, 2 and 3. The fin pitches are approximate 1.2 and 1.8 mm. As shown in the figure, influence of the number of tube row on the friction factors are relatively small. This phenomenon is observed for most highly interrupted surfaces. Basic heat transfer characteristics of the present fin geometry in conjunction with the effect of the tube row are summarized as follows:

1. For $Re_{Dc} < 1000$, higher heat transfer performance is seen for $N = 1$ in comparison with multiple number of tube row. However, one can see that the characteristics is reversed when $Re_{Dc} > 1000$. The heat transfer performance for $N = 1$ is slightly lower than those of having multiple rows and the difference increases with increase of the Reynolds number. Apparently, this is due to the additional vortex shedding caused by the blockage of the tube row.
2. For dense fin pitches like $F_p = 1.2$ mm at $Re_{Dc} < 1000$, the heat transfer performance drops very sharply with the number of tube row. The results can be interpreted from the observations by Mochizuki et al. [9] who reported steady laminar flow patterns prevailed throughout the core for offset slit geometry at low Reynolds number region. This implies that the heat transfer performances may deteriorate significantly as the depth of the core is increased.

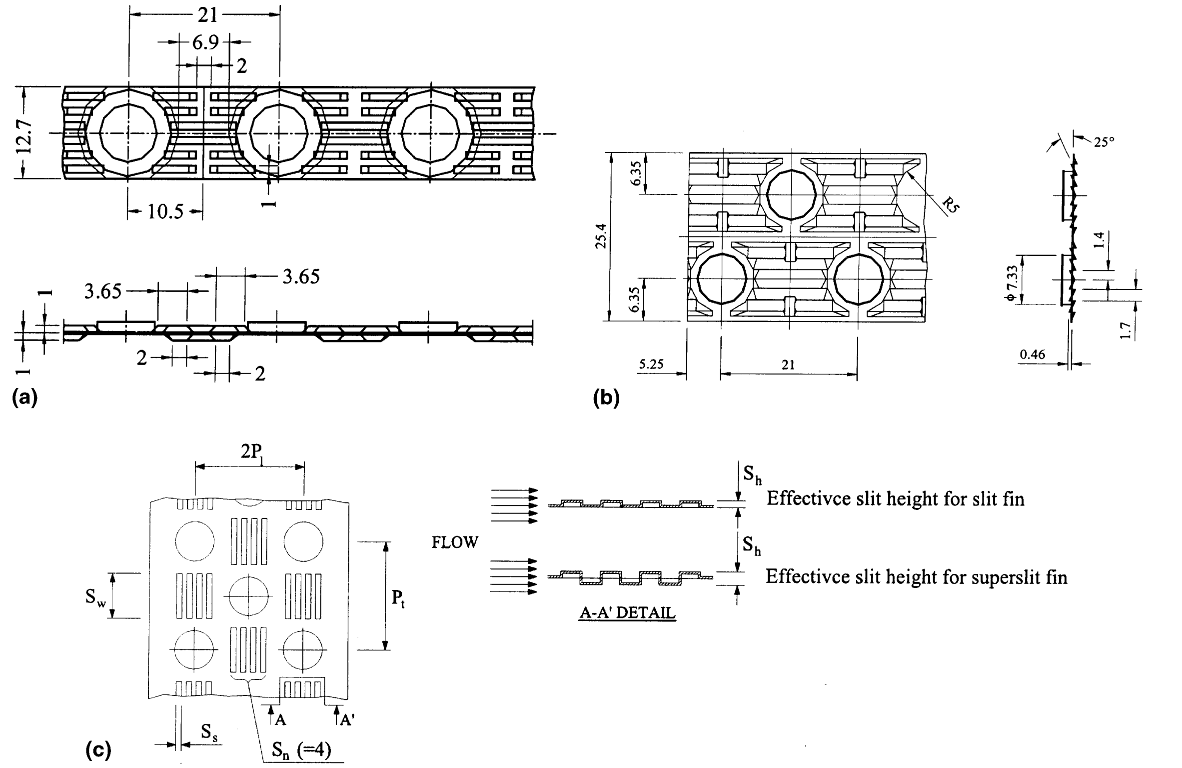

Fig. 1. Details of the present slit fin geometry and related terminology of the slit fin geometry. (a) Present slit fin; (b) lower fin; (c) definition of slit fin.

3. For multiple row configuration ($N > 1$), the effect of the number of tube row is very small when $Re_{\mathrm{Dc}} > 1000$. Observations of Fig. 2 reveal that the effect of tube row and the fin pitch on the heat transfer performance is almost negligible. Again, this phenomenon can be explained from those observations by Mochizuki et al. [9]. They reported that as the Reynolds number reached a significantly high value, the turbulent intensity became nearly uniform throughout the core. This phenomenon is especially pronounced for offset slit fin geometry having smaller fin length.

Based on the present test results and those reported by previous investigators [3–5], an updated correlation for the airside performance is proposed. Regression was performed for a total 56 samples of slit fin-and-tube heat exchangers. The data bank contains approximately 530 data points. The proposed correlations for the Coburn j factors and Fanning friction factors f are given as follows:

$$j = \begin{cases} 0.9047 Re_{\mathrm{Dc}}^{j1} \left(\frac{F_s}{D_c}\right)^{j2} \left(\frac{P_t}{P_l}\right)^{j3} \left(\frac{S_s}{S_h}\right)^{-0.0305} N^{0.0782} \\ \qquad \text{for } N > 2 \text{ and } Re_{\mathrm{Dc}} < 700, \\ j = 1.0691 Re_{\mathrm{Dc}}^{j4} \left(\frac{F_s}{D_c}\right)^{j5} \left(\frac{S_s}{S_h}\right)^{j6} N^{j7} \\ \qquad \text{for } N = 1, 2 \text{ or } N > 2 \text{ and } Re_{\mathrm{Dc}} > 700, \end{cases} \tag{1}$$

$$f = 1.201 Re_{\mathrm{Dc}}^{f1} \left(\frac{F_s}{D_C}\right)^{f2} \left(\frac{P_t}{P_l}\right)^{f3} \left(\frac{S_s}{S_h}\right)^{f4} (N)^{f5} (S_n)^{f6}, \tag{2}$$

where

$$j1 = -0.2555 - \frac{0.0312}{(F_s/D_c)} - 0.0487N, \tag{3}$$

$$j2 = 0.9703 - 0.0455\sqrt{Re_{\mathrm{Dc}}} - 0.4986\left(\ln\frac{P_t}{P_l}\right)^2, \tag{4}$$

$$j3 = 0.2405 - 0.003\,Re + 5.5349\left(\frac{F_s}{D_c}\right), \tag{5}$$

$$j4 = -0.535 + 0.017\left(\frac{P_t}{P_l}\right) - 0.0107N, \tag{6}$$

$$j5 = 0.4115 + 5.5756\sqrt{\frac{N}{Re_{\mathrm{Dc}}}}\ln\frac{N}{Re_{\mathrm{Dc}}} + 24.2028\sqrt{\frac{N}{Re_{\mathrm{Dc}}}}, \tag{7}$$

$$j6 = 0.2646 + 1.0491\left(\frac{S_s}{S_h}\right)\ln\frac{S_s}{S_h} - 0.216\left(\frac{S_s}{S_h}\right)^3, \tag{8}$$

Table 1
Geometric dimensions of the slit fin-and-tube heat exchangers

No.	References	F_p (mm)	D_c (mm)	P_t (mm)	P_l (mm)	δ_f (mm)	N	S_h (mm)	S_s (mm)	S_n	No. of j data	No. of f data
1	This study	1.27	7.6	21	12.7	0.115	1	2	1	6	10	10
2	This study	1.81	7.6	21	12.7	0.115	1	2	1	6	10	10
3	This study	1.21	7.6	21	12.7	0.115	2	2	1	6	10	10
4	This study	1.81	7.6	21	12.7	0.115	2	2	1	6	10	10
5	This study	1.27	7.6	21	12.7	0.115	3	2	1	6	10	10
6	This study	1.81	7.6	21	12.7	0.115	3	2	1	6	10	10
7	Wang et al. [5]	1.48	10.32	25	21.65	0.11	1	1.46	1.98	7	10	10
8	Wang et al. [5]	1.71	10.32	25	21.65	0.11	1	1.46	1.98	7	9	9
9	Wang et al. [5]	1.88	10.32	25	21.65	0.11	1	1.46	1.98	7	9	9
10	Wang et al. [5]	2.10	10.32	25	21.65	0.11	1	1.46	1.98	7	9	9
11	Wang et al. [5]	2.24	10.32	25	21.65	0.11	1	1.46	1.98	7	10	10
12	Wang et al. [5]	2.50	10.32	25	21.65	0.11	1	1.46	1.98	7	10	10
13	Wang et al. [5]	1.51	10.32	25	21.65	0.11	2	1.46	1.98	7	10	10
14	Wang et al. [5]	1.71	10.32	25	21.65	0.11	2	1.46	1.98	7	10	10
15	Wang et al. [5]	1.87	10.32	25	21.65	0.11	2	1.46	1.98	7	10	10
16	Wang et al. [5]	2.11	10.32	25	21.65	0.11	2	1.46	1.98	7	10	10
17	Wang et al. [5]	2.30	10.32	25	21.65	0.11	2	1.46	1.98	7	10	10
18	Wang et al. [5]	2.50	10.32	25	21.65	0.11	2	1.46	1.98	7	10	10
19	Wang et al. [5]	1.51	10.32	25	21.65	0.11	3	1.46	1.98	7	10	10
20	Wang et al. [5]	1.70	10.32	25	21.65	0.11	3	1.46	1.98	7	10	10
21	Wang et al. [5]	1.88	10.32	25	21.65	0.11	3	1.46	1.98	7	10	10
22	Wang et al. [5]	2.10	10.32	25	21.65	0.11	3	1.46	1.98	7	10	10
23	Wang et al. [5]	2.50	10.32	25	21.65	0.11	3	1.46	1.98	7	10	10
24	Wang et al. [5]	1.51	10.32	25	21.65	0.11	4	1.46	1.98	7	10	10
25	Wang et al. [5]	1.70	10.32	25	21.65	0.11	4	1.46	1.98	7	9	9
26	Wang et al. [5]	1.92	10.32	25	21.65	0.11	4	1.46	1.98	7	10	10
27	Wang et al. [5]	2.10	10.32	25	21.65	0.11	4	1.46	1.98	7	10	10
28	Wang et al. [5]	2.50	10.32	25	21.65	0.11	4	1.46	1.98	7	9	9
29	Wang et al. [5]	1.20	7.52	20	17.32	0.11	1	1.6	1	7	11	11

30	Wang et al. [5]	1.40	7.52	20	17.32	0.11	1	1.6	1	7	11	11
31	Wang et al. [5]	1.60	7.52	20	17.32	0.11	1	1.6	1	7	11	11
32	Wang et al. [5]	1.20	7.52	20	17.32	0.11	2	1.6	1	7	11	11
33	Wang et al. [5]	1.40	7.52	20	17.32	0.11	2	1.6	1	7	11	11
34	Wang et al. [5]	1.60	7.52	20	17.32	0.11	2	1.6	1	7	11	11
35	Wang et al. [5]	1.20	7.52	20	17.32	0.11	3	1.6	1	7	10	10
36	Wang et al. [5]	1.40	7.52	20	17.32	0.11	3	1.6	1	7	11	11
37	Wang et al. [5]	1.60	7.52	20	17.32	0.11	3	1.6	1	7	11	11
38	Wang et al. [4]	1.28	10.34	25.4	22	0.12	1	0.99	2.2	4	10	10
39	Wang et al. [4]	1.76	10.34	25.4	22	0.12	1	0.99	2.2	4	10	10
40	Wang et al. [4]	2.43	10.34	25.4	22	0.12	1	0.99	2.2	4	10	10
41	Wang et al. [4]	1.21	10.34	25.4	22	0.12	2	0.99	2.2	4	10	10
42	Wang et al. [4]	1.79	10.34	25.4	22	0.12	2	0.99	2.2	4	10	10
43	Wang et al. [4]	2.46	10.34	25.4	22	0.12	2	0.99	2.2	4	10	10
44	Wang et al. [4]	1.22	10.34	25.4	22	0.12	4	0.99	2.2	4	10	10
45	Wang et al. [4]	1.22	10.34	25.4	22	0.12	4	0.99	2.2	4	10	10
46	Wang et al. [4]	2.47	10.34	25.4	22	0.12	4	0.99	2.2	4	11	11
47	Wang et al. [4]	1.21	10.34	25.4	22	0.12	6	0.99	2.2	4	9	9
48	Wang et al. [4]	1.78	10.34	25.4	22	0.12	6	0.99	2.2	4	10	10
49	Wang et al. [4]	2.48	10.34	25.4	22	0.12	6	0.99	2.2	4	10	10
50	Nakayama and Xu [3]	2.00	16.30	38	33	0.15	2	1	2	3	0	7
51	Nakayama and Xu [3]	1.70	16.30	38	33	0.15	2	1	2	3	0	5
52	Nakayama and Xu [3]	2.50	16.30	38	33	0.15	2	1	2	3	0	4
53	Nakayama and Xu [3]	2.50	16.4	38	33	0.18	2	1	2	3	12	0
54	Nakayama and Xu [3]	1.90	9.90	25	22	0.2	2	1	2	4	0	7
55	Nakayama and Xu [3]	2.50	9.90	25	22	0.2	2	1	2	4	0	10
56	Nakayama and Xu [3]	2.00	8.4	28	15	0.2	6	1	2	4	4	0
Number of data used to develop correlation											509	526

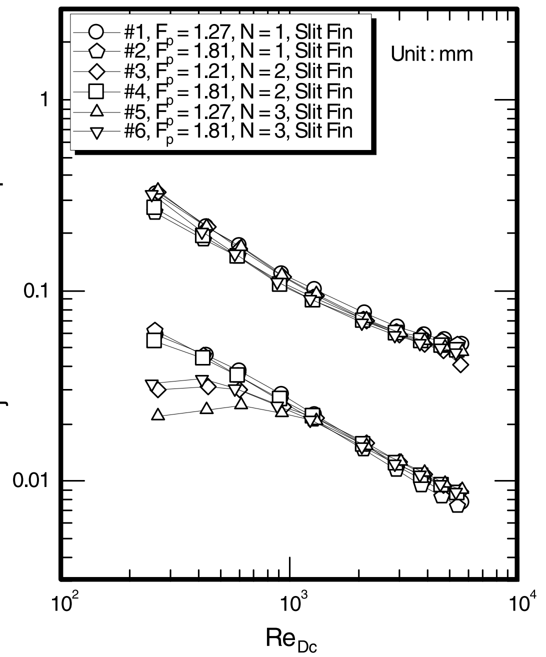

Fig. 2. j and f vs. Re_{Dc} for the present compact slit fin geometry.

$$j7 = 0.3749 + 0.0046\sqrt{Re_{\mathrm{Dc}}}\ln Re_{\mathrm{Dc}} - 0.0433\sqrt{Re_{\mathrm{Dc}}} \tag{9}$$

$$f1 = -0.1401 + 0.2567\ln\left(\frac{F_\mathrm{s}}{D_\mathrm{c}}\right) + 4.399\,\mathrm{e}^{-S_n}, \tag{10}$$

$$f2 = -0.383 + 0.7998\ln\left(\frac{F_\mathrm{s}}{D_\mathrm{c}}\right) + \frac{5.1772}{S_n}, \tag{11}$$

$$f3 = -1.7266 - 0.1102\ln(Re_{\mathrm{Dc}}) - 1.4501\left(\frac{F_\mathrm{s}}{D_\mathrm{c}}\right), \tag{12}$$

$$f4 = 0.4034 - 0.199\left(\frac{S_\mathrm{s}/S_\mathrm{h}}{\ln(S_\mathrm{s}/S_\mathrm{h})}\right) + 0.4208\left(\frac{\ln(S_\mathrm{s}/S_\mathrm{h})}{(S_\mathrm{s}/S_\mathrm{h})^2}\right), \tag{13}$$

$$f5 = -9.0566 + 0.6199\ln Re_{\mathrm{Dc}} + \frac{32.8057}{\ln Re_{\mathrm{Dc}}} - \frac{0.2881}{\ln N} + \frac{0.9583}{N^{1.5}}, \tag{14}$$

$$f6 = -1.4994 + 1.209\left(\frac{P_\mathrm{t}}{P_\mathrm{l}}\right) + \frac{1.4601}{S_n}. \tag{15}$$

The present Eq. (1) can describe 90.2% of the j factors within 15% while Eq. (2) can correlate 90.7% of the friction factors within 15%. The mean deviation of Eq. (1) is 7.26% and for Eq. (2) is 7.18%.

A large different methods had been proposed for facilitating comparison, and these methods have been summarized by Shah [10]. The comparison methods were identified as four categories in Shah's review, namely,

1. Direct comparison of j and f.
2. Comparison of heat transfer as a function of fluid power.
3. Performance comparison with a reference surface.
4. Miscellaneous comparison method.

For an initial screening and selection of the surface, Shah [10] recommended:

1. j/f vs. Re is recommended for flow ''area goodness'' comparison.
2. h_{std} vs. E_{std} is recommended for selecting a surface where there are no system or manufacturing restraints.
3. $\eta_\mathrm{o} h_{\mathrm{std}}\beta$ vs. $E_{\mathrm{std}}\beta$ characterizes a surface as best from a ''volume goodness'' viewpoint.
4. The performance evaluation method by Bergles et al. [11] is recommended for other design criteria.

For detailed comparison of the performance of the present compact slit fin geometry, enhanced surface (louver fin, Fig. 1(b)) was adopted from Wang et al. [2] as competitive surface. The basic reference surface is the plain fin surface that was taken from Wang and Chi [12]. Notice that the related surfaces are of similar configuration ($P_\mathrm{t} = 21$ mm, $P_\mathrm{l} = 12.7$ mm, $D_\mathrm{c} = 7.5$–7.6 mm, and $N = 2$). For the first stage of the comparison, direct comparisons of the corresponding j and f are made. It is found that the both heat transfer and friction performance are comparable for louver and slit fin geometry. For the same fin pitch, the heat transfer performance for interrupted surfaces are about 30–50% higher than that of plain fin surface when $Re_{\mathrm{Dh}} > 200$. The results are quite surprising since one may expect the louver fin may outperform that of slit fin geometry. Notice that the louver angle is 25° and the slit height is 1.0 mm. The previous study [4] showed that the heat transfer enhancement relative to plain fin is only near 10–15%. Hence, a close examination of previous investigation was made. The results reveal that the major differences are attributable to the number of effective slit and slit breadth (the slit height are comparable for this study and that of previous one, 1.0 and 0.99 mm). Notice that the previous study contains a slit breadth of 2.2 mm comparing to 1mm of this study. For the offset parallel-plate surfaces, Mochizuki et al. [9] showed that the turbulence intensity can be significantly improved by decreasing the slit breadth. For $S_\mathrm{s}/S_\mathrm{h} = 0.75$, the turbulence intensity is about 25–50% higher than that of $S_\mathrm{s}/S_\mathrm{h} = 1.5$. They concluded that the turbulence intensity increases with decrease of slit breadth. In view of this phenomenon, one may expect a much higher heat transfer performance for the present slit geometry. Thus, the effect of slit breadth may be more important than the slit height in practical design.

Fig. 3 shows the comparison of the interrupted surfaces (including louver and slit) and the corresponding plain fin surface by use volume goodness method for $F_p = 1.2$ mm. Notice that the volume goodness factor was suggested by Kays and London [13], and is given as below:

$$\eta_o h_{std}\beta = \frac{c_p \mu}{Pr^{2/3}} \eta_o \frac{4\sigma}{D_h^2} j\ Re, \tag{16}$$

$$E_{std}\beta = \frac{\mu^3}{2 g_c \rho^2} \frac{4\sigma}{D_h^4} f\ Re^3, \tag{17}$$

where $\eta_o h_{std}\beta$ represents the heat transfer power per unit temperature difference and per unit core volume; $E_{std}\beta$ represents the friction power expenditure per unit core volume. The subscripts "std" is any preferred standard condition for comparison. From the range of standard rating condition of a heat exchanger as depicted by ARI [14], the standard condition was selected at 35°C, 1 atm. A "high" plot on $\eta_o h_{std}\beta$ vs. $E_{std}\beta$ characterizes that surface as best from the viewpoint of heat exchanger volume required. Geometries having large values of $\eta_o h_{std}\beta$ will require the least core volume for a given airside performance. As shown in Fig. 3, performance of the present slit fin and louver fin geometry is comparable. For a given $E_{std}\beta$ ($E_{std}\beta = 1000$), the $\eta_o h_{std}\beta$ value of interrupted surfaces about 15–20% higher than that of plain fin. It should be pointed out that there is no detectable differences among slit, louver and plain fin when $E_{std}\beta < 200$ which suggests that it may be not beneficial for enhanced surfaces to operate at the low velocity region. A further increase of fin pitch to 1.8 mm, results of $\eta_o h_{std}\beta$ vs. $E_{std}\beta$ are shown in Fig. 4. Unlike those appeared in Fig. 3, one can see that the interrupted surfaces are much more effective than that in small fin pitch. Actually, for $E_{std}\beta = 1000$, the $\eta_o h_{std}\beta$ value of interrupted surfaces are about 50% higher than that of plain fin.

For a detailed comparison of the benefits of using enhanced fins, the VG-1 criteria performance criteria had been adopted, for which relevant description can be found from Webb [15]. The VG-1 criteria seeks the possibility of reduction of surface area by using enhanced fin surface having fixed pumping power, heat duty, and temperature difference. Fig. 5 shows the benefits of using interrupted surfaces. As seen, surface reduction is attainable by use of the enhanced surfaces. It should be noted that the A/A_{ref} shows a lowest value near $500 < Re_{Dh} < 1000$. The results implies that the interrupted surfaces are especially beneficial at 2 m/s $< V_{fr} < 4.0$ m/s. Approximately 45% area reduction was seen for the slit fin geometry ($N = 2, F_p = 1.81$ mm) near $Re_{Dh,ref} = 500$, It is also noted that for the same reference Reynolds number, larger area reduction is

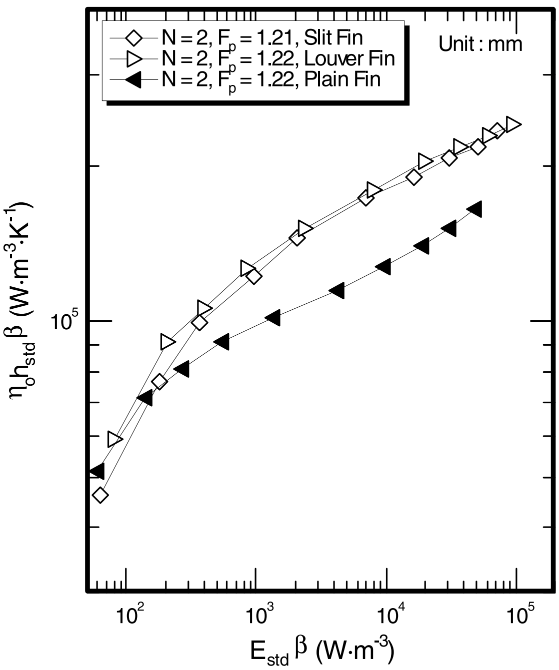

Fig. 3. Volume goodness comparison with $F_p \approx 1.2$ mm and $N = 2$.

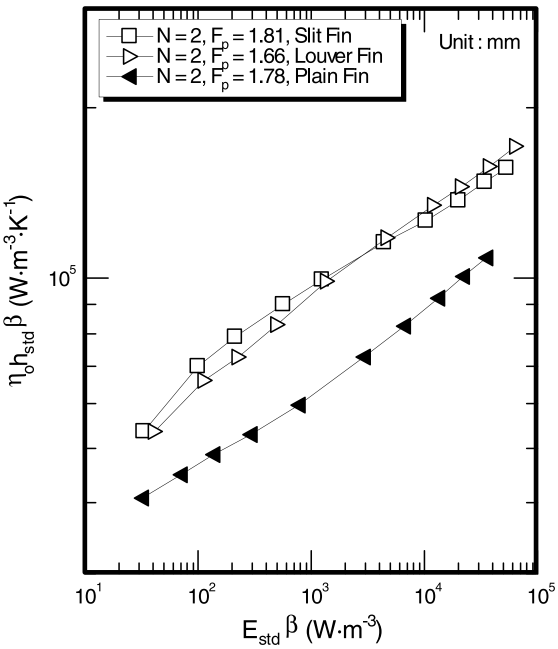

Fig. 4. Volume goodness comparison with $F_p \approx 1.8$ mm and $N = 2$.

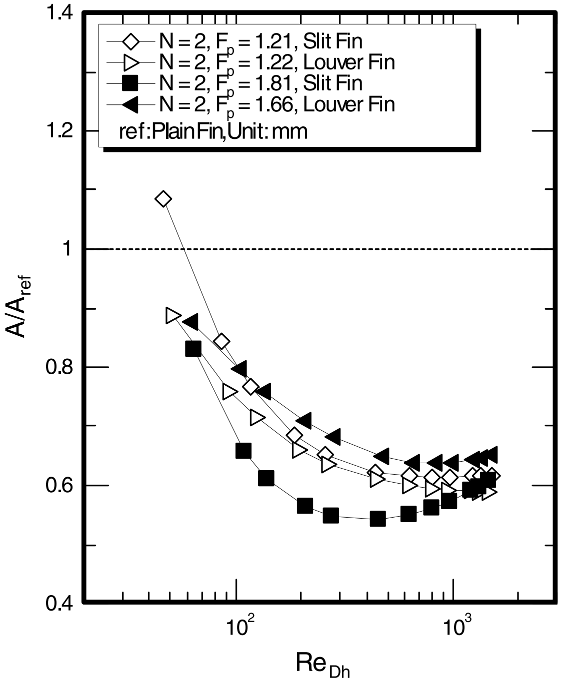

Fig. 5. Area reduction ratio for interrupted surfaces using VG-1 criterion.

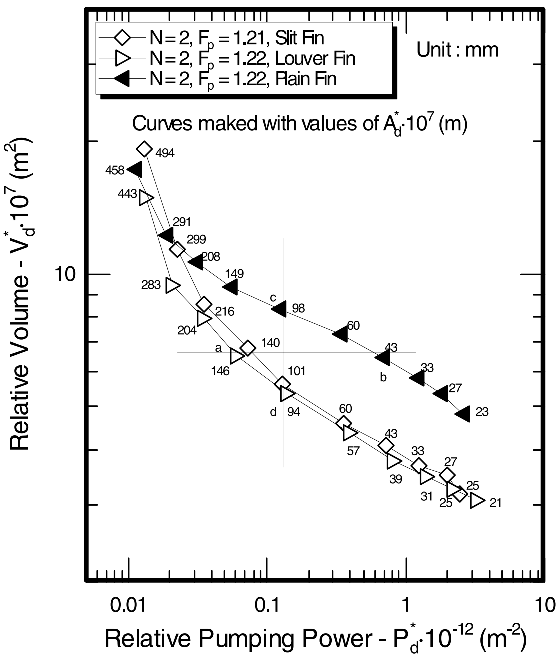

Fig. 6. Relative volume plotted against relative pumping power at fixed scale and constant heat transfer.

likely for larger fin pitch. Notice that the reference surface is the plain fin having the same fin pitch.

In addition to the conventional comparison methods, Cowell [16] presents a family of methods for comparing compact heat transfer surface configurations. He shows that the relative values of required hydraulic diameter, frontal area, total volume, pumping power, and number of transfer units can be derived and displayed, when any two of the above five parameters are held constant. Following the terminology derived from Cowell [16], for any heat transfer duty, the values of the relative frontal area, relative volume, and relative pumping power of the particular surfaces are

$$A_d^* = \frac{d}{\sigma\, Re}, \tag{18}$$

$$V_d^* = \frac{d^2}{\sigma j\, Re}, \tag{19}$$

$$P_d^* = \frac{f\, Re^2}{jd^2}. \tag{20}$$

The suffix d indicates that parameters are for fixed hydraulic diameter for any particular surface and the asterisk indicates the part of the parameter associated with the particular solution.

For each of the surfaces to be compared, the "relative pumping power", P_d^*, can be plotted against "relative volume" V_d^* and the curves marked with the corresponding value with the corresponding values of "relative frontal area" A_d^*. Fig. 6 shows curves plotted for the test heat exchangers having $F_p = 1.21$ mm. For the slit and louver fin surface, it can be seen that for a given total volume (e.g., $V_d^* = 6.5 \times 10^{-7}$, points (a) and (b)), the plain fin surface will have a pumping power approximately 10 times higher than those of the slit and louver fin surfaces, but the frontal area will be smaller by a factor of near 30% relative to the interrupted surfaces. For the three surfaces to perform the required duty with the same pumping power, (e.g., for $P_d^* = 0.13 \times 10^{12}$, points (c) and (d)) the ratio of the relative volumes for the plain fin surface will be approximately 50% higher than those of interrupted surfaces, and with frontal area ratio approximately the same. For the same frontal area (e.g., $A_d^* = 43 \times 10^{-7}$) the heat exchanger volume for the interrupted surfaces will be smaller by a factor 38% relative to plain fin surface.

4. Conclusions

The present authors conduct an experimental study on the airside performances of compact slit fin-and-tube heat exchangers provide related comparisons with louver and plain fin surface. Conclusions can be summarized as follows.

- The effect of the number of tube row on the frictional performance for the present compact slit fin

geometry is relatively small. Influence of the fin pitch on the heat transfer performance is also relatively small for $Re_{\mathrm{Dc}} > 1000$. For the same fin pitch, the heat transfer performance for $N = 1$ and $Re_{\mathrm{Dc}} < 1000$ is higher than those of multiple-row configuration, However, the trend is slightly reversed when $Re_{\mathrm{Dc}} > 3000$.
- The slit breadth plays a significant role in improving the heat transfer performance when comparing to the effect of slit height.
- The proposed heat transfer correlation can describe 90.2% of the j factors within 15% while the frictional correlation can correlate 90.7% of the friction factors within 15%. The mean deviation of heat transfer correlation is 7.26% and for friction correlation is 7.18%.
- Various comparison methods were made to compare the airside performance among louver, slit, and plain fin. For the geometry investigated, it is found that the slit and louver fin are comparable. In all cases, the relevant airside performance for interrupted surfaces is superior to plain fin surface. However, it should be pointed out that the associated superiority may be lost with decrease of fin pitch and the Reynolds number.

Acknowledgements

The financial support of this work is provided by the Energy R&D foundation funding from the Energy Commission of the Ministry of Economic Affairs, Taiwan.

References

[1] C.C. Wang, Recent progress on the airside performance of fin-and-tube heat exchangers, Int. J. Heat Exchangers 1 (2000) 49–76.
[2] C.C. Wang, C.J. Lee, C.T. Chang, S.P. Lin, Heat transfer and friction correlation for compact louvered fin-and-tube heat exchangers, Int. J. Heat Mass Transfer 42 (1999) 1945–1956.
[3] W. Nakayama, L.P. Xu, Enhanced fins for air-cooled heat exchangers heat transfer and friction correlations, in: Proceeding of the First ASME/JSME Thermal Engineering Joint Conference, vol. 1, 1983, pp. 495–502.
[4] C.C. Wang, W.H. Tao, C.J. Chang, An investigation of the airside performance of the slit fin-and-tube heat exchangers, Int. J. Refrigeration 22 (1999) 595–603.
[5] Y.J. Du, C.C. Wang, An experimental study of the airside performance of the superslit fin-and-tube heat exchangers, Int. J. Heat Mass Transfer 43 (2000) 4475–4482.
[6] C.C. Wang, Y.M. Tsi, D.C. Lu, Comprehensive study of convex-louver and wavy fin-and-tube heat exchangers, AIAA J. Thermophys. Heat Transfer 12 (1998) 423–430.
[7] C.C. Wang, R.L. Webb, K.U. Chi, Data reduction for airside performance of fin-and-tube heat exchangers, Experiment. Therm. Fluid Sci. 21 (2000) 218–226.
[8] R.J. Moffat, Describing the uncertainties in experimental results, Experiment. Therm. Fluid Sci. 1 (1988) 3–17.
[9] S. Mochizuki, Y. Yagi, W.J. Yang, Flow pattern and turbulence intensity in stacks of interrupted parallel surfaces, Experiment. Therm. Fluid Sci. 1 (1988) 51–57.
[10] R.K. Shah, Compact heat exchanger surface selection methods, in: Proceedings of the Sixth International Heat Transfer Conference, vol. 4, Toronto, 1978, pp. 193–199.
[11] A.E. Bergles, A.R. Blumenkrantz, J. Taborek, Performance evaluation criteria for enhanced heat transfer surfaces, in: Proceedings of the Fourth International Heat Transfer Conference vol. 2, 1974, pp. 239–243.
[12] C.C. Wang, K.U. Chi, Heat transfer and friction characteristics of plain fin-and-tube heat exchangers: part I: new experimental data, Int. J. Heat Mass Transfer 43 (2000) 2681–2691.
[13] W.M. Kays, A.L. London, Trans. ASME 72 (1950) 1087–1097.
[14] ARI Standard 410, Standard for Forced Circulation Air-Cooling and Air-Heating Coils, 1981, Air-Conditioning and Refrigeration Institute, Arlington, VA.
[15] R.L. Webb, in: Principles of Enhanced Heat Transfer, Wiley, New York, 1994.
[16] T.A. Cowell, A general method for the comparison of compact heat transfer surfaces, ASME J. Heat Transfer 112 (1990) 288–294.